2023

Effect of Molecular Crowders on the Activation of Cholera Toxin by Protein Disulfide Isomerase

Niral Shah
University of Central Florida

THE EFFECT OF MOLECULAR CROWDERS ON THE ACTIVATION OF CHOLERA TOXIN BY PROTEIN DISULFIDE ISOMERASE

by

NIRAL SHAH
UCF, 2023

A thesis submitted in partial fulfillment of the requirements
for the Honors Undergraduate Thesis Program in Molecular and Cellular Biology
in the College of Medicine
and in The Burnett Honors College
at the University of Central Florida
Orlando, Florida

Spring Term
2023

Thesis Chair: Dr. Ken Teter

ABSTRACT

Cholera toxin (CT) is a classic A-B type protein toxin that has an A subunit (A1 + A2) and a pentameric B subunit. The catalytic A1 domain is linked to the A2 domain via a disulfide linkage. CTA1 must be dissociated from the rest of the toxin to cause a cytopathic effect. Protein disulfide isomerase (PDI) can reduce the CTA1/CTA2 disulfide bond, but disassembly of the reduced toxin requires the partial unfolding of PDI that occurs when it binds to CTA1. This unfolding event allows PDI to push CTA1 away from the rest of the toxin.

My research question is whether the efficiency of PDI in disassembling CT would be affected by molecular crowding, where a dense internal cell environment is recreated in vitro by the use of chemical agents such as Ficoll. This will give insight on how CT behaves inside a cell. Our hypothesis was that molecular crowding would make CTA1 disassembly more efficient by recreating the tight packing of macromolecules in cells, which provides an extra nudge to enhance toxin disassembly. We then used enzyme-linked immunosorbent assays (ELISAs), a pull-down assay and a biochemical assay to determine how molecular crowders affect the binding, reduction, and disassembly of CT by PDI. Our results will bring about a deeper understanding of the cellular events that may affect the course of a cholera infection.

From the preliminary results, molecular crowders increased PDI's ability to bind to CTA1 and did not prevent PDI from cleaving the CTA1/CTA2 disulfide bond. Based off the

disassembly results, molecular crowders reduced PDI's ability to displace CTA1 from the rest of the toxin. This contradicts our original hypothesis. Our new hypothesis is that crowders block PDI unfolding, which is required for CT disassembly. Biophysical experiments using Fourier Transform Infrared Spectroscopy will test this prediction in future work.

ACKNOWLEDGMENTS

For my mentor, Dr. Teter, for your continuous support and guidance throughout the past two years during the GEAR and HUT programs. It has been a joy to work in your lab, always receive feedback from you, and help me carve a path to my future. Thank you for giving me the opportunity to experience the rewards of taking part in research.

For my family, for being “behind-the-scenes” reason for success. You know how much it means to me.

Table of Contents

LIST OF FIGURES

INTRODUCTION

Cholera

Cholera is an acute infection caused by the bacterium *Vibrio cholerae* that is transmitted by the consumption of food or water that has been contaminated by feces[1]. Approximately 1 in 10 people infected by cholera can develop severe symptoms, which include rice-water stools and vomiting. If left untreated, the massive loss of fluid and electrolytes can cause electrolyte imbalance, dehydration, and shock. As of 2015, around 2.8 million people were infected annually with cholera and, out of those, roughly 91,000 people died[2]. One of the major sources of infection is limited access to safe drinking water and clean sanitary practices [3, 4]. Therefore, cholera disproportionally affects developing countries that don't have adequate sewage and water treatment facilities[1]. Refugee camps are affected by cholera due to them being densely populated, lack of clean water, and poor hygiene and sanitation practices[5]. For example, in 2016 Dadaab, a refugee camp in Kenya, experienced the largest cholera outbreaks with an attack rate of 5.1 per 1000. The leading cause of the outbreak was food markets being proximally located to an area with poor water drainage[6]. To add on, most of the inhabitants of refugee camps are typically malnourished, hence outbreaks of cholera are prevalent[5]. The risk of cholera outbreaks is heightened after natural disasters, such as earthquakes or floods. Regions with lack of clean water are hit the worst, such as overcrowded temporary shelters. Lack of sanitation management and clean water is what allows the rapid progression of cholera infections[7]. Cholera became endemic to Haiti after the 2010 earthquake, where *Vibrio cholerae* was unintentionally introduced into the country and claimed the lives of 10,000

people. This is a perfect example of how vulnerable countries with limited resources can face massive outbreaks following natural disasters[8].

AB Toxins

Many bacteria secrete AB type toxins composed of an A subunit, which is the enzymatic component and a B subunit that is the cell binding component. This allows these toxins to reach the intracellular compartment and target host machinery, which contributes to pathogenicity[9]. AB toxins include heat-labile toxin (LT) produced by enterotoxigenic *Escherichia coli* (ETEC), Shiga toxin (ST) produced by *Shigella dysenteriae* and some *Escherichia coli* strains, cholera toxin (CT) from *Vibrio cholerae* and more[10]. These toxins cross a membrane to reach the cytosol. There are some AB toxins that are transported through acidified endosomes. As the acidity of the endosome increases, the B subunit undergoes a conformational change which is inserted into the endosomal membrane. This forms a pore and allows the A subunit to translocate into the cytosol[11, 12]. Other AB toxins travel through endosomes but lack acid-triggered pore-forming capacity and instead use retrograde transport to move through the trans Golgi network (TGN) before reaching the endoplasmic reticulum (ER). The ER has an exiting pore that allows the toxin to reach the cytosol[10, 13]. The focus of this thesis will be cholera toxin.

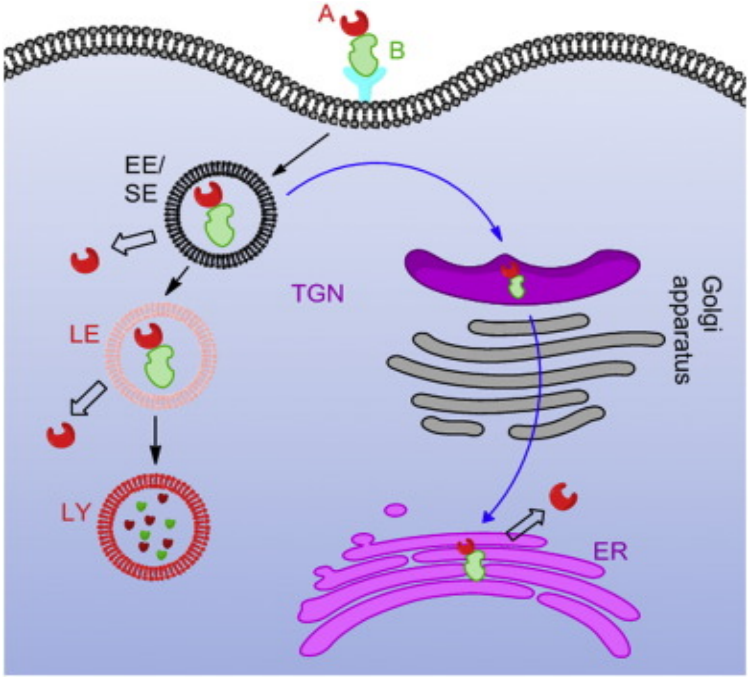

Figure 1: schematic showing routes AB toxins take to gain access to the cytosol.
All AB toxins must cross a membrane barrier to gain access to the cytosol. The cell binding B subunit binds to cell membrane to enter the cell, and the AB toxin gets packaged into an early endosome, EE. Some of the AB toxins move from the endosomes to the Golgi apparatus and other toxins can translocate across the EE/SE (sorting endosome) or LE (late endosome). The majority of toxin moves through the endosomal system and is degraded in the lysosomes (LY). Source: https://www.sciencedirect.com/journal/advanced-drug-delivery-reviews

Cholera Toxin

Cholera toxin (CT) is secreted by the bacterium *Vibrio cholerae*, a Gram-negative pathogen, within the intestinal lumen initiating a cascade of events that lead to toxin activation. CT (Fig. 2) is an AB type toxin, composed of the catalytic A1 domain, an A2 linker, and the cell binding pentameric B subunit that is organized in a ring like structure. It is the CTA2 linker that connects CTA1 to CTB_5[14, 15]. Initially, CT is composed of a single A subunit (CTA) and the pentameric B subunit[16-18]. CTA has an intramolecular disulfide bond and is nicked by serine-like bacterial or host proteases to form CTA1 and CTA2 polypeptides linked together by the disulfide bridge[17-19]. This proteolytic nicking is required for toxin unfolding and activation[20]. As a holotoxin, CT is inactive.

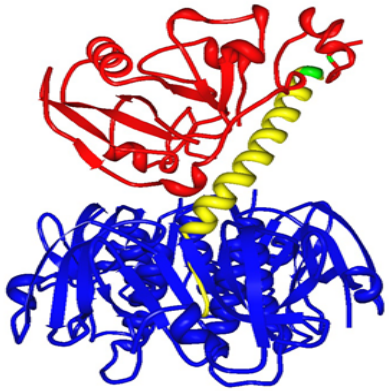

Figure 2: crystal structure of CT. red represents the A1 domain, yellow represents the A2 linker, green represents the disulfide bond, and blue represents the pentameric B subunit. PDB: 1S5F

Activation of Cholera Toxin

The activation process of CT begins when CTB_5 adheres to GM1 ganglioside receptors that are distributed on the surface of intestinal epithelial cells (Fig. 3). CT enters the cell via endocytosis and is transported retrograde through the *trans*-Golgi network (TGN) to eventually reach the ER[15, 21]. The redox environment of the ER although oxidizing, breaks the disulfide bond between A1/A2[19]. However, this doesn't promote toxin activation[22]. Chaperone assisted disassembly will push CTA1 away from the rest of the holotoxin[20, 23]. Free CTA1 spontaneously unfolds in the ER, and heat-shock proteins (Hsps) recognize

them and mediate host ER-associated degradation (ERAD) pathway to retro-translocate into the cytosol[24, 25]. ERAD is a process that transports misfolded proteins into the cytosol for degradation by proteasomes[21, 22, 24, 26]. First, the chaperone protein Hsp40 recognizes the misfolded protein, and transfers it to another chaperone protein, Hsp70. Hsp40 stimulates hydrolysis of the ATP on Hsp70 into ADP so that Hsp70 can have a higher affinity for the substrate[22, 25]. BiP, a Hsp70 chaperone protein, interacts with CTA1 by masking the hydrophobic patches, therefore preventing its aggregation while being transported through the Sec61 channel to reach the cytosol[22, 25, 27]. Furthermore, Hsp90 is also required for the extraction of CTA1 from the ER into the cytosol. As soon as CTA1 exits into the cytosol, it escapes proteasomal degradation because it lacks lysine residues that would have allowed ubiquitin to bind[24, 28, 29]. Instead, CTA1 has many arginine residues[22, 29]. Furthermore, the reason why the toxin avoids degradation is not only the lack of lysines, but also because Hsp90 remains bound to CTA1, which assists CTA1 to refold into a stable conformation[22, 24, 28-30]. The now functional CTA1 adds an ADP-ribose to the alpha subunit of a G-protein (Gsα), making it permanently active by preventing its bound GTP from being hydrolyzed to GDP[31]. The activated Gsα activates adenylyl cyclase, which produces cAMP from ATP[22, 32, 33]. cAMP binds to inactive PKA, activating it, which then phosphorylates cystic fibrosis transmembrane conductance regulator (CTFR). The result of this is a massive loss of chloride ions into the intestinal lumen (Fig. 3)[22, 33]. To restore the osmotic balance, huge amounts of water and electrolytes are

secreted into the intestinal lumen[4]. Therefore, the characteristic symptom of a severe cholera infection is rice-water stools.

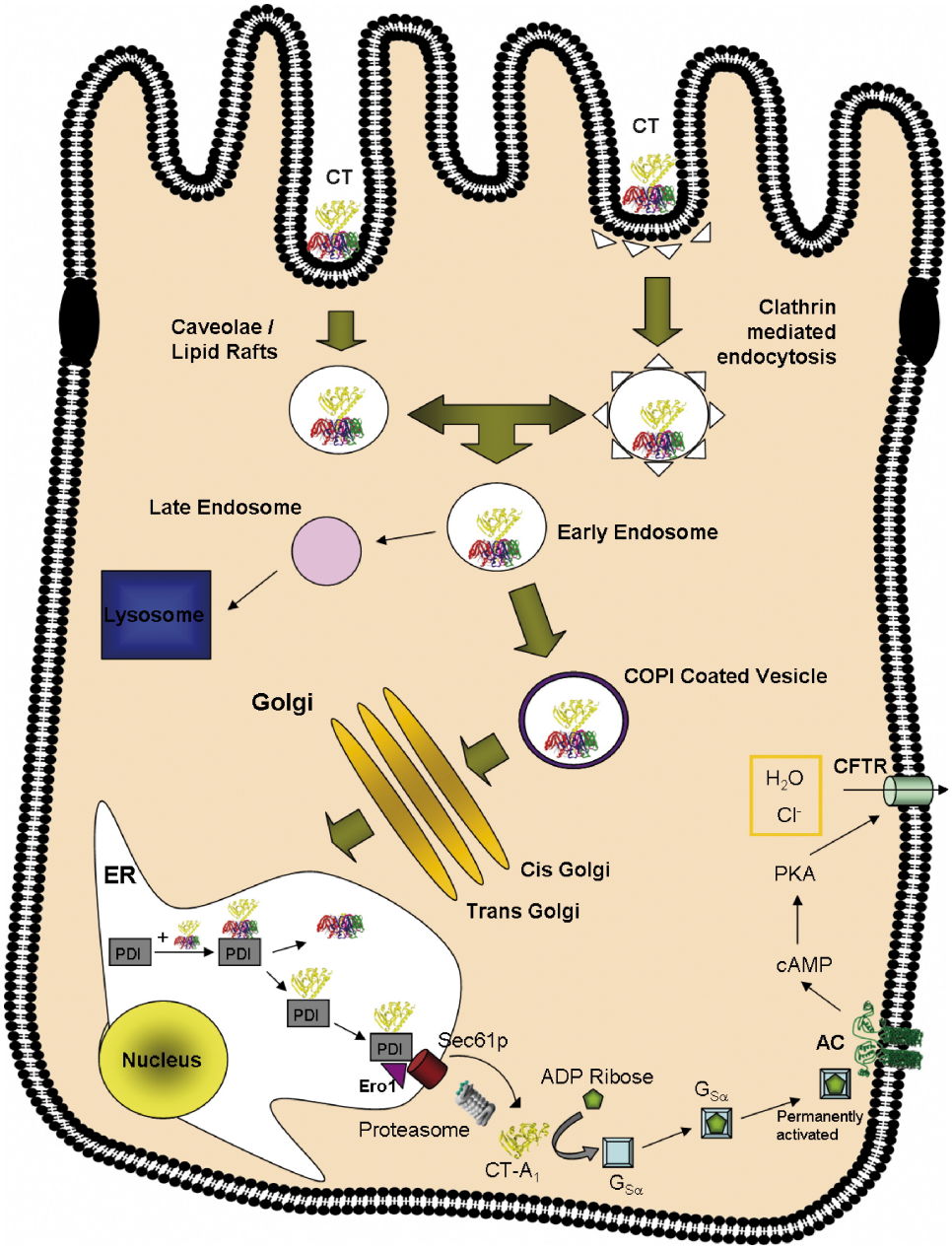

Figure 3: CT cell entry and intoxication. CTB binds to GM1 gangliosides on the surface of target cell. Endocytosis of CT allows its further transport to the ER, where it encounters protein disulfide isomerase (PDI). PDI disassembles CT, releasing CTA1, which is transported as a misfolded protein to the cytosol where it refolds. The now functional CTA1 ADP-ribosylates the alpha subunit of the heterotrimeric G-protein(Gsα), making it permanently active. Gsα binds to adenylyl cyclase, which makes cAMP from ATP. The cAMP binds to inactive protein kinase A (PKA), activating it. PKA phosphorylates cystic fibrosis transmembrane conductance regulator (CFTR) which pumps chloride ions into the intestinal lumen. Water is pumped into the lumen to restore the osmotic balance, resulting in severe diarrhea. Source: https://www.sciencedirect.com/science/article/pii/S1357272507002208

Chaperone Proteins in the Endoplasmic Reticulum

The ER is a major protein hub, where selected proteins are translated and folded before being transported to reach target destinations. In addition, the ER is also the major site of quality control, where only correctly folded proteins are allowed to leave to the Golgi. Many proteins made by the ribosome have a signal peptide that serves as an address to be mailed to the ER. A signal recognition particle (SRP) binds to the signal peptide, as well as the ribosome, pausing translation, and causing this complex to bind to an SPR receptor (SR) located on the ER[34]. Translation resumes as the protein moves through a pore into the lumen of the ER [34, 35]. After entering the ER lumen the signal peptide is cleaved off a water soluble protein[36, 37]. The nascent proteins will then be guided to attain their respective conformation by the aid of chaperone proteins[34]. Otherwise, they stand a chance to misfold or aggregate. Molecular chaperones help other polypeptides to attain their native conformation without being part of the polypeptide structure[36].

There are many chaperones found in the ER. For example, Hsp70 and Hsp90 families (ATP binding proteins) are usually upregulated in the presence of heat shock or other ER stressors[30]. They recognize misfolded, or aggregation prone proteins by the presence of exposed hydrophobic residues on native proteins[36]. Another type of chaperone proteins are ER folding enzymes. They catalyze reactions during folding, without changing the equilibrium of the reaction[36]. A maturing nascent protein can undergo oxidative folding when ER folding enzymes bind and assist the formation of proper disulfide bond pairs in the protein[38]. For example, protein disulfide isomerase (PDI) is a unique protein because

it is not only an oxidoreductase folding enzyme, but also a chaperone protein[39]. It is involved in the formation, isomerization, or reduction of disulfide bonds respective to the conditions[35, 36, 40, 41]. Once the correct conformation is reached, chaperone proteins let go of the client protein, which is subsequently packaged in vesicles to be directed to other locations. Only fully folded and functional proteins are allowed to leave the ER. Or else, they will be retained in the ER by chaperone proteins[36].

ER Homeostasis, ERAD and UPR

Protein folding isn't always perfect, therefore a proper process of degrading them must be present. Otherwise, these misfolded proteins will be trapped within the ER, disrupting ER homeostasis through aggregate formation. One process of disposing these proteins is ER-associated degradation (ERAD), where terminally misfolded proteins are recognized and transported into the cytosol for degradation by the ubiquitin-proteosome system[42, 43]. Covalent attachment of the C-terminus of ubiquitin to an internal lysine residue, as well as formation of a polyubiquitin tail via ubiquitin-ubiquitin linkages marks the protein for degradation (Fig. 4)[44]. However, if ERAD

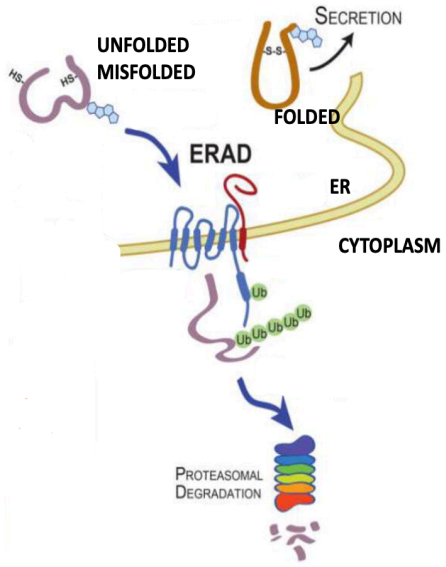

Figure 4: schematic showing ERAD process. Properly folded proteins are secreted out of the ER. Terminally misfolded proteins are disposed out of the ER via ERAD by being transported into the cytosol to be degraded by proteosomes. Source: PMC5440201

doesn't work, the unfolded protein response (UPR) takes place to restore ER homeostasis. UPR works by 1) reducing the number of proteins entering the ER, 2) increasing the capacity of the ER to fold proteins, and 3) removing unfolded proteins that take longer to fold through enhanced ERAD. All these mechanisms help to reduce ER stress[45].

Protein Disulfide Isomerase

Foldases speed up the folding of proteins by catalyzing rate limiting steps, such as formation, isomerization, and reduction of disulfide bonds. Chaperone proteins bind to proteins to prevent misfolding or aggregation[39]. They also help the ER cope with stress by transporting misfolded proteins to the cytosol to be degraded by proteosomes. A well-known redox-dependent chaperone protein that is a foldase as well as a chaperone, is PDI. The crystal structure of PDI (Fig. 5) shows four thioredoxin-like domains, aa'bb', taking the shape of a twisted U conformation. The catalytic a and a' domains are situated at the top of the U, facing each other[46]. The substrate binding b and b' domains are located on the inside of the U (Fig. 5). When PDI is in an oxidized state (in normal steady-state conditions), all 4 domains are in the same plane. But when PDI is in a reduced state (activating isomerase properties), the abb' are in the same plane and the a' domain is twisted, almost like a hook. Therefore,

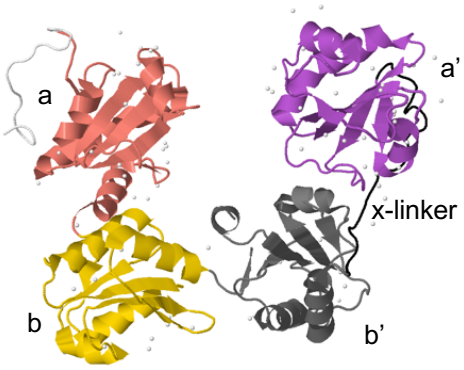

Figure 5: crystal structure of PDI. Pink and purple represent a and a' catalytic domains; yellow and black represent b and b' cell binding domains; and the x linker is between a' and b'. Source: PDB 4EKZ

the redox state determines its activity as an enzyme[46]. It catalyzes disulfide bond formation or reduction by accepting or donating electrons (Fig. 6)[47].

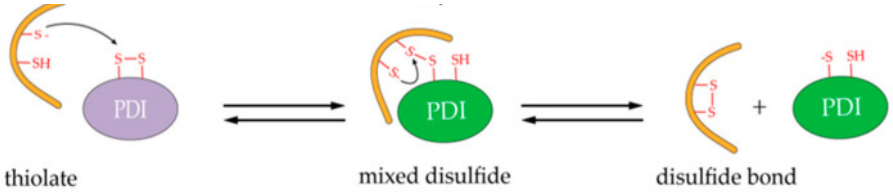

Figure 6: Oxidoreductase properties of PDI. In this schematic, reduced PDI (green) has sulfhydryl groups that can accept electrons from a substrate protein (yellow, far right) to reduce the disulfide bond, becoming oxidized itself (purple). Source: doi:10.3390/molecules26010171

For many substrates, the redox state of PDI does not matter when it binds to various polypeptides. However, its chaperone activity is enhanced when its active site in the a' domain is in an oxidized state (allowing for a more open conformation). PDI without cysteine residues in its active site won't be a functional enzyme, but it can still bind to proteins that don't have thiol groups present showing that its chaperone properties are intact. The chaperone activity of PDI is complimentary to its oxidoreductase properties[48].

PDI and CT Interaction

When CT enters the ER, reduced PDI recognizes the folded confirmation of CTA1, which is still bound to the holotoxin[49]. PDI binds to it and unfolds, pushing CTA1 away from the rest of the holotoxin[50]. CTA1 on its own is highly unstable and immediately unfolds (Fig. 7), while PDI regains its native conformation[50]. It should be noted that PDI does not unfold CTA1, but rather physiological temperature causes the unfolding event[49, 50]. PDI-CTA1 interaction is unique because PDI can normally bind to unfolded proteins, but in this

situation, PDI will only recognize the folded conformation of CTA1[49]. It is known that the action of PDI leads to the cellular potency of CT because cells that are PDI-deficient are resistant to intoxication[22].

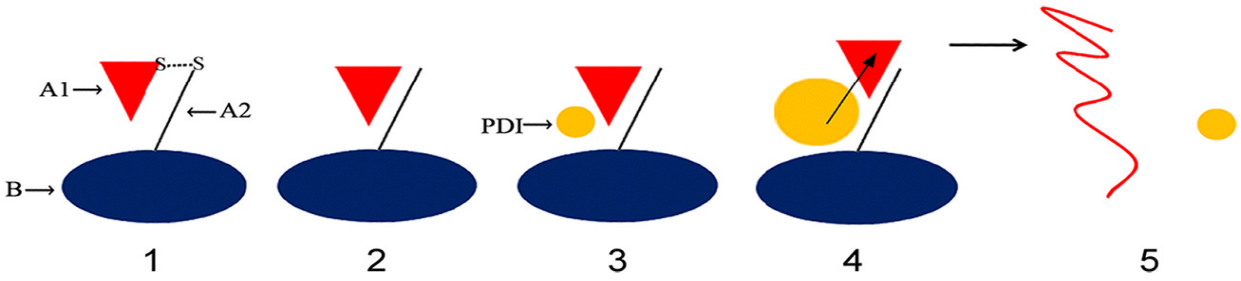

Figure 7: Disassembly of CTA1 by PDI. CT holotoxin enters the ER, where its disulfide bond is reduced. After this event CTA1 keeps its connection to the rest of the holotoxin. Reduced PDI identifies this toxin, unfolds, and acts as a wedge to displace CTA1 from the rest of the holotoxin. Free CTA1 spontaneously unfolds and is recognized as a misfolded whereby it follows the mechanisms of ERAD. Reduced PDI regains its native conformation. Source: https://doi.org/10.1016/j.cellsig.2022.110489

There are agents that prevent PDI from unfolding, such as EDC and ribostamycin. It has been reported that PDI treated with these agents can bind to CT. However, it is unable to unfold and cannot disassemble CTA1, which provides support for it acting as a wedge to push CTA1 from the rest of the holotoxin[50].

After its release from CTA2/CTB_5, CTA1 is recognized as a misfolded protein by the binding of Hsp40, which then transfers CTA1 to BiP, an ER localized Hsp70 protein. This process initiates the ERAD mechanism. BiP is released and Hsp90 binds to CTA1 at the cytosolic face of the ER membrane pore, allowing its export through the pore to reach the cytosol from the ER. As soon as the N-terminus of CTA1 is exposed to the cytosol, hydrolysis of ATP on Hsp90 guides the refolding of CTA1 to its proper active conformation[22, 30, 36]. It should be emphasized that it is the lack of lysine residues that

allows CTA1 to escape proteasomal degradation[28]. This is how CTA1 exploits the ERAD mechanism for toxin activation[21, 26].

Previous Experiments That Showcase CT Disassembly by PDI

We have previously documented PDI-driven CT disassembly by 2 methods, enzyme-linked immunosorbent assay (ELISA) and surface plasmon resonance (SPR). ELISA showed 10%-20% disassembly within 1 hour, but the SPR assay showed complete disassembly in approximately 10 minutes or less. The difference is present because ELISA is a more static procedure, where the proteins are sitting in a well waiting for an interaction to occur. On the other hand, SPR uses a perfusion chamber that moves fluid over the proteins in questions. This movement of fluid over the proteins provides an extra nudge to promote toxin disassembly that ELISA isn't able to provide. Maybe SPR is able to promote efficient disassembly by mimicking what is happening in the ER. Therefore, to improve the ELISA experiments, I looked for conditions that would replicate the push that the perfusion buffer is able to provide in SPR. Molecular crowding agents seem to provide that.

Molecular Crowding

The interactions between CT and PDI have been studied in an in vitro environment made of dilute buffers, but how these interactions occur in a cellular environment is still obscure. The inside of a cell is much more different than in vitro conditions[51]. Cells are crowded compartments, filled with various macromolecules that could cause steric hinderance and bring opportunities for specific or non-specific interactions with other molecules[52, 53]. Many

proteins must wade their way around macromolecules to find their binding partners to carry out a biological function. Just like we control temperature or pH in experiments, it would seem wise to recreate the crowded cellular environment. This would enable one to understand protein-protein interactions from a physiological aspect and gain a deeper understanding of biological processes in a living cell.

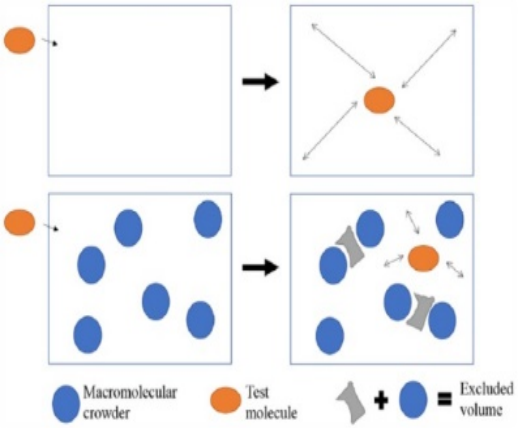

Figure 8: In vitro vs. in vivo conditions. In vitro environments allow molecules to freely diffuse. However, in a crowded environment, the test molecules don't diffuse freely. Source: doi:10.1177/2041731417730467

It was known that cellular environments are crowded, rather than concentrated since early 1960's[54]. Each single macromolecule in the cell is at a low concentration, but combining all macromolecules together forms a crowded environment. However, the use of molecular crowding agents didn't appear until around 1993, when scientists wanted to recreate internal cellular environments[56]. Molecular crowding agents are inert, whereby they simply occupy solvent space. They limit the proteins in question from occupying space without interacting with the proteins and cause some degree of steric hinderance (Fig. 8).The commonly used molecular crowders are chemicals that are inert, non-charged polymers with different sizes, such as Ficoll, polyethylene glycol (PEG) and sucrose[53, 56].

SPECIFIC AIMS

The goal of this project is to recreate cellular conditions in vitro using molecular crowding agents. The hypothesis was that molecular crowders would enhance disassembly of CTA1 by PDI because the crowders would enhance the physical push that PDI uses to wedge CTA1 away from the holotoxin. Furthermore, other PDI-CT interactions would remain unaffected in the presence of molecular crowding agents. To test the proposed hypothesis, enzyme-linked immunosorbent assays (ELISA) were carried out to determine how well PDI can bind to CT and disassemble CTA1 in the presence of molecular crowders. To determine if other PDI-CTA1 interactions are affected or not, a reducing environment was created and a non-reducing SDS-PAGE was run to visualize if PDI was able to break the disulfide bond between CTA1 and CTA2.

There were 3 different aims to collect evidence towards the hypothesis, as indicated below:

Aim 1: Investigating the Efficiency of PDI Binding to CT in the Presence of Molecular Crowders

Disassembly begins when reduced PDI binds to CT. To quantify the binding event, binding assays were conducted to determine if PDI binds to CT in the presence of molecular crowders. If binding is achieved, only then can PDI help dislodge CTA1 from the rest of the holotoxin.

Aim 2: Investigating if Molecular Crowders Affect CT Reduction by PDI

When PDI is in a reduced state, its conformation slightly changes allowing it to interact with CT. This interaction can break the disulfide bond between CTA1/A2. To explore PDI's

ability to accept electrons from CT and break the sulfur bridge, a reducing environment was created that only reduced PDI and not CT directly. A non-reducing SDS-PAGE was run to visualize if CTA1/A2 has been reduced or not by PDI with or without molecular crowders present. This gave us an idea if molecular crowders affect another important PDI – CT interaction.

Aim 3: Investigating the Effect of Molecular Crowders on Disassembling CTA1 by PDI

Activation of CT occurs when the catalytic domain, CTA1 has been disassembled from the rest of the holotoxin. ELISA-based disassembly assays were run to quantitatively determine how efficiently PDI can dislodge CTA1 in the presence of molecular crowders. This gives us a clue if CTA1 disassembly in the ER is an efficient process or not.

Once a person is intoxicated with CT, the only treatment at the present is to run the course of infection and remain hydrated. That being said, the long-term goal of this project is to understand PDI-CT interactions within the ER, and to hopefully create a therapeutic cure that prevents CT disassembly, which prevents its activation. This type of therapeutic would be targeted to people who already have been exposed to the toxin.

MATERIALS AND METHODS

Enzyme Linked Immunosorbent Assays (ELISAs)

Binding Assay

Protein A plates were washed three times with 100 μL of phosphate-buffered saline containing 0.05% Tween 20 (PBS-T). Next, 100 μL of 1:1,500 dilution of polyclonal PDI antibody in 2.5% bovine serum albumin (BSA)/PBS-T was prepared and loaded into the wells of a 96-well plate and allowed to be captured for 60 minutes at 4°C. The plate was washed three times with PBS-T before adding 100 μL 2.5% BSA/PBST and allowed to incubate overnight. The next day, the liquid from the wells was dumped out and 100 μL pre-reduced 20 μg/mL PDI in PBS-T with 2.5% BSA and dithiothreitol (DTT) was added. For the background, PBS-T with 2.5% BSA and DTT alone were added. The plate was allowed to incubate for 1 hour at 4°C. The PDI is pre-reduced using DTT to ensure it is in the correct conformation when captured by the PDI-antibody. Thereafter, 100 μL (550 ng/well) of CTA1 conjugated to horseradish peroxidase (HRP) in a specific molecular crowder condition was added to the respective wells. The plate was left at 4°C for 1 hour. This is the step that assesses whether CTA1 can find its binding partner (PDI) in the presence of molecular crowders. After 6 washes with 200 μL PBST, 100 μL of TMB substrate was added and allowed to incubate in the dark for 5-10 minutes before adding the stop solution (2N H_2SO_4). The absorbance was measured at 450 nm. The percent of toxin binding was calculated as a percentage of CTA1-HRP binding to PDI in the absence of crowders. The procedure is summarized in Fig. 9.

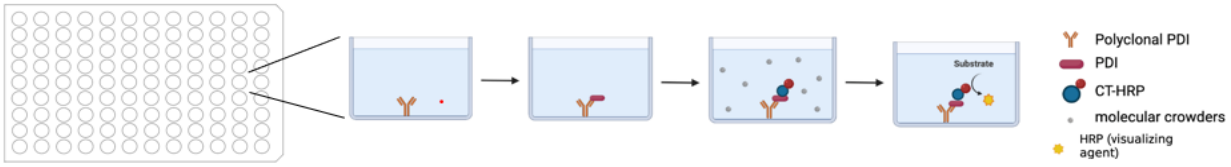

Figure 9: ELISA binding assay schematic. The wells of a 96-well plate were first coated with polyclonal PDI antibody so that PDI can be captured to the wells in the next step. This is followed by the addition of HRP-CTA1 in the presence of molecular crowders. Lastly, the substrate TMB is added and after 5 min, stop solution is added. The absorbance is measured at 450 nn and percent binding is calculated. Made using Biorender.

Disassembly Assay

50 μL of 6 μg/mL of GM1 in ethanol was added to the wells of the plate and was allowed to air dry overnight at room temperature. The plates were then washed with PBS-T before adding 100 μL of 1 μg/mL CT in PBS-T with 2.5% BSA. After 1 hour at 4°C, all the wells were washed with PBS-T. Next, the wells were incubated with pre-reduced 20 μg/ml PDI in PBS-T with the specific molecular crowder and DTT or, for the control, PBS-T with the specific crowder and DTT alone. Another control with no molecular crowder was present, where 2.5% BSA in PBS-T was added. The plate was left at room temperature for 1 hour, followed by PBS-T washes and then the addition of anti-CTA1 primary antibody (100 μL at 1:1000 dilution) for 1 hour at 4°C. This was followed by another set of PBS-T washes and the addition of HRP-conjugated goat anti-rabbit antibody (100 μL at 1:5000 dilution) for 30 min. TMB substrate was added for 5-10 minutes before adding the stop solution (2N H_2SO_4) and the absorbance was measured at 450 nm. The percent of toxin disassembly was calculated. A loss of signal indicates that disassembly occurred. The procedure is summarized in Fig. 10.

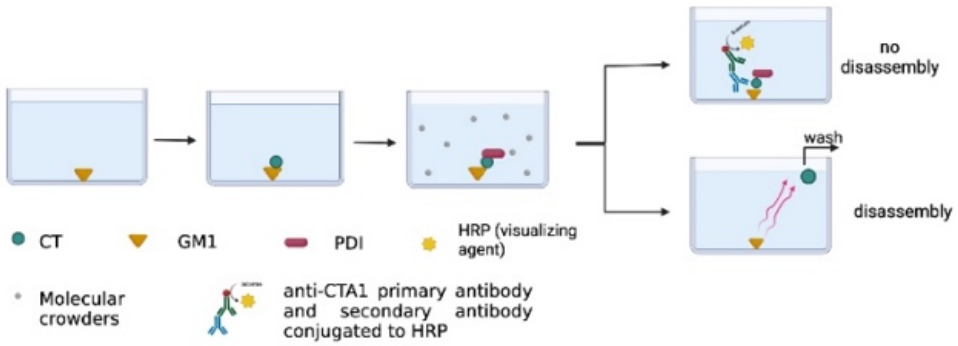

Figure 10: ELISA disassembly assay schematic. The wells of a 96-well plate were first coated with GM1 so that CT can be captured to the wells in the next step. This is followed by the addition of PDI in the presence of molecular crowders. Next, anti-CTA1 primary antibody is added, followed by HRP-secondary antibody. Lastly, the substrate TMB is added and after 5 min, stop solution is added. The absorbance is measured at 450 nn and percent disassembly is calculated.

Reduction Assay

NADPH, Trx and TR were added to a microcentrifuge tube. This creates a series of redox reactions so that when PDI is added it can donate elections to reduce PDI (Fig. 11). CTA is added next, but the solution can't reduce the disulfide bond in CTA as determined by control experiments. This allows PDI to use its oxidoreductase properties to reduce the CTA disulfide bond. The mixture of 333 μM NADPH, 213 nM Trx, 53 nM TR, 3 μM PDI, 1.3 μM CTA and specific molecular crowder are incubated at 37 °C for four hours. To visualize if CTA is reduced, a 15% SDS-PAGE was cast and the samples were run under non-reducing conditions. The molecular weights of the different bands (26 kDa for CTA and 21 kDa for CTA1) allowed for interpretation of the results.

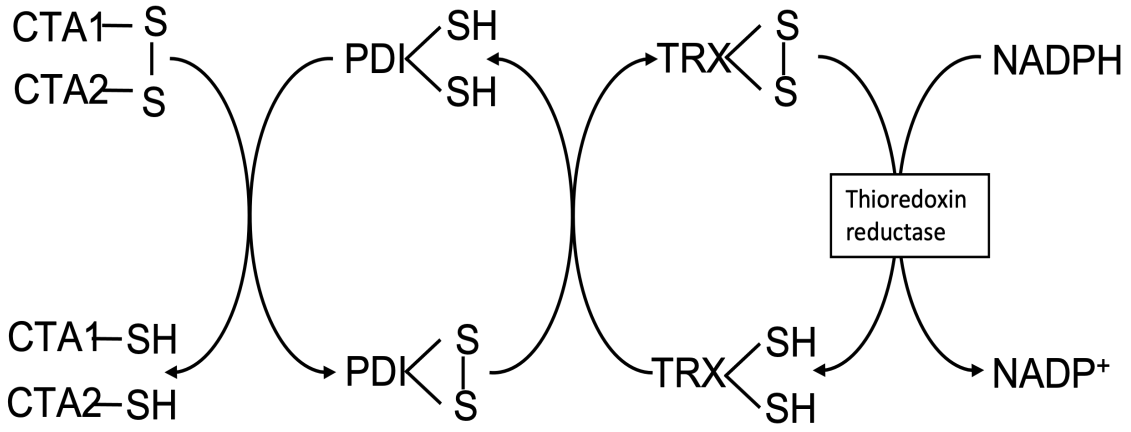

Figure 11: PDI reduction using thioredoxin. In this chain of redox reaction, PDI can easily convert between an oxidized and reduced state. This allows PDI to form and reduce disulfide bonds in substrate proteins, in this case the disulfide bonds between CTA1 and CTA2. Made by Dr. Robb Hunh.

Pull-down assay

1 mL buffer (0.5% BSA/PBS) was added to 50 μL of Talon beads and the sample was centrifuged at 5000 rpm for 2 minutes. The supernatant was discarded, and the pellet was resuspended in 1 mL buffer. The washes were repeated twice. Next, the pellet was resuspended in 1 ml buffer containing 1 μg His-tagged CTA and was incubated for 1 hour at 4°C. Thereafter, the sample was washed 4 times in 1 mL buffer. This was followed by the addition of 9 μg PDI (no His-tag present) in mL buffer and one sample was incubated for 1 hour while another sample was incubated for 24 hours at 4°C. For a control, PDI alone with the Talon beads were incubated for 1 hour or 24 hours at 4°C. Next, the samples were centrifuged at 5000 rpm for 2 minutes.

The supernatant from the samples containing CTA1 and PDI was kept. 10% TCA was added and incubated at 4°C for 10 minutes, followed by centrifugation at 16000 rpm for

5 minutes. The supernatant was discarded, and the pellet was washed twice in ice cold acetone. The pellet was resuspended in 50 μL 1X SB.

The pellets of the two timepoints, CTA1 + PDI and PDI alone, were washed 4 times in 1 mL buffer. The pellets were then resuspended in 50 μL 1X SB. 20 μL of the samples were loaded into two SDS-PAGE gels. One gel had His-tagged CTA1 controls (10 ng and 100 ng CTA) and excluded PDI only samples. The other gel had all samples, as well as PDI controls (10 ng and 100 ng PDI). After completing western transfers, the CTA1 blot was incubated in 1:5000 anti-CTA1 antibody and the PDI blot was incubated in 1:5000 anti-PDI antibody. The blots were incubated overnight, covered at 4°C. Next, the blots were washed 3 times in TBS-T, 5 minutes each, followed by the addition of 1:20000 goat anti-rabbit secondary antibody for incubation at room temperature for 30 minutes. The blots were washed 3 times in TBS-T and luminescence solution was added as a visualization agent. The procedure is summarized in Fig. 12.

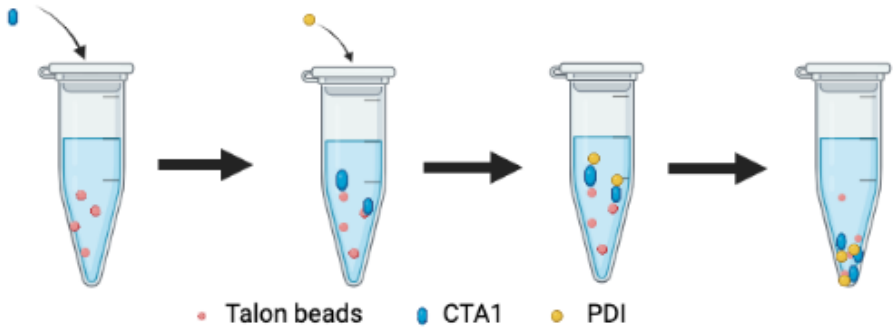

Figure 12: simplified schematic of pull-down: Talon beads and buffer (PBS/0.5%BSA) are washed three times, followed by the addition of his-tagged CTA1. After 1 hour, PDI is added and allowed to bind to CTA1. The samples are washed four times and resuspended in sample buffer. An SDS-PAGE gel is cast, followed by a western blot. Made using Biorender.

RESULTS AND DISCUSSION

ELISA Binding Assay

This assay quantified the percent binding of PDI to CTA1 in the presence of various molecular crowders, and the results were compared to the control condition of no molecular crowders. Our initial hypothesis was that molecular crowding agents would allow for more successful interactions between PDI and CT. This is because there are more molecules in the solution, hence the higher the likelihood of collisions. Therefore, the chance of a successful interaction is higher.

A 96 well plate was coated with a polyclonal PDI antibody to capture PDI in the wells. HRP conjugated CTA1 was added next. This is the step where molecular crowders are added, which potentially impact how well CTA1 can bind to the captured PDI. The HRP is an enzyme, where the addition of its substrate helped quantify the binding signal through the generation of a colored product. A preliminary experiment reported 5% PEG improved binding the most, followed by 1% PEG and then Ficoll (Fig. 13). 5% PEG contains more molecules, as compared to 5% Ficoll. This is because the molecular weight of Ficoll is approximately 400,000 g/mol, while that of PEG is 3350 g/mol. Therefore, a more crowded environment was created in 5% PEG which corresponded to more collisions in general. This allowed for a higher chance for PDI and CTA1 to bind. 5% Ficoll and 1% PEG seemed to showcase a similar crowded environment since their results are almost identical. On the contrary, sucrose inhibited binding since its percent binding is less than the control. Overall, preliminary data showcased that a crowded environment in

the ER may enhance PDI-CT binding event. More repeats for this experiment need to be done to establish reproducibility.

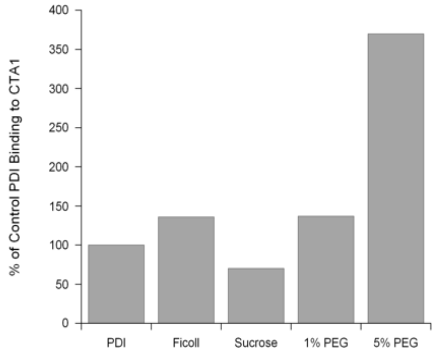

Figure 13: ELISA binding assay. PDI was captured on the wells of a PDI-antibody coated ELISA plate. CT was added in the presence of the various molecular crowders, or with no crowders for the control. It's already known that PDI binds to CT in vitro, hence this control was set to 100% binding. All the other conditions were compared to this.

Pull-down assay

A secondary experiment to ELISA binding assay is the pull-down assay. A pull-down assay investigates protein-protein interaction, where the first protein is allowed to bind to beads, followed by the addition and pull down of another protein due to protein-protein interactions. The purpose of secondary experiments strengthens data, where similar results from different methods verifies the observed results.

In this protocol, Talon beads were used to capture His-tagged CTA1. This was followed by the addition of PDI. The blots determine whether CTA1 can pulldown PDI.

CTA1 blot

10ng and 100 ng CTA1 are controls to show that the protein present is CTA1. CTA1 is not present in the TCA, showing that most of the CTA1 present is bound to the Talon beads. CTA1 + PDI at the different time points show that CTA1 was bound to the Talon beads (Fig. 14).

PDI blot

10ng and 100 ng PDI are controls to show that the protein is present. CTA1 + PDI 1 hour barely showed a band, meaning that 1 hour may not be enough time to capture PDI. The TCA 1 hour sample had PDI present because PDI was present in the supernatant rather than being bound to CTA1. CTA1 + PDI 24 hours had a band present showing that CTA1 managed to pull down PDI. The TCA 24 hours sample had PDI present, showing that the pulldown wasn't very efficient. To our surprise, PDI alone samples had bands present, showing that non-specific binding was present (Fig. 14). That being said, we can't be sure if PDI was bound to CTA1 or the beads. Future experiments will be conducted to inhibit non-specific binding of PDI to the Talon beads, followed by pull-down assays with the molecular crowders present.

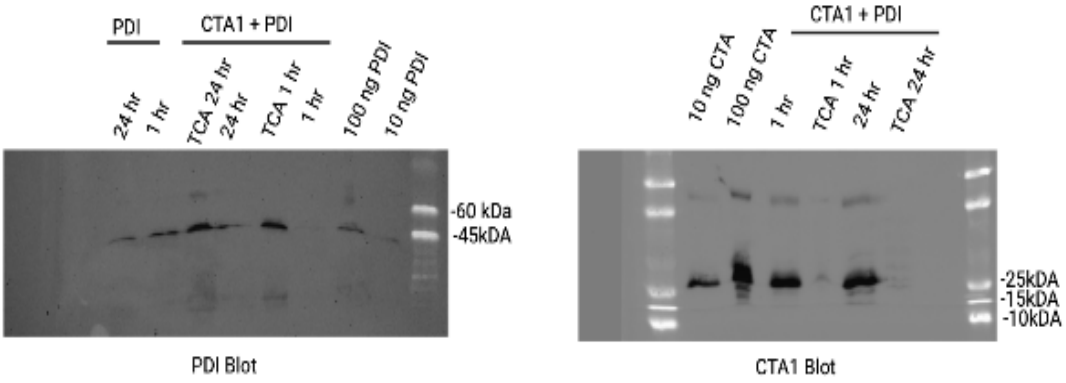

Figure 14: pull-down of PDI by CTA1: his-tagged CTA1 was allowed to bind to talon beads, and followed by the addition of PDI. The samples were incubated at either 1 hour or 24 hours. **Right panel:** CTA1 blot shows that it his-tagged CTA1 was bound to talon beads under different conditions. Protein samples of 10ng and 100 ng CTA1 was added to verify CTA1 was present. **Left panel**: the PDI blot shows that PDI bound to CTA1 in the various conditions. PDI alone control was present to show that PDI has a low affinity for the talon beads. The results suggest that CTA1 can pull down PDI. Non-specific binding with PDI and talon beads is present. More experiments are to be conducted

Reduction Assay for the Disulfide Bond Linking CTA1/A2

Physiologically, the disulfide bond linking CTA1 and CTA2 is reduced in the ER. However, an environment can be created where only PDI can be oxidized or reduced, and not CT (Fig. 11). In this case, PDI uses its chaperone properties to accept electrons from the disulfide bond in CTA1/A2 and reduce it [47, 48]. This is the basis for the next research goal: finding out if molecular crowders affect CTA reduction by PDI. Reduction of CTA was studied by incubating it with PDI that is coupled with NADPH, thioredoxin (trx) and thioredoxin reductase (TR)[57]. CTA, TR, trx and PDI were incubated with the different molecular crowders. The controls we had were CTA alone, reduced CTA, CTA with PDI, and CTA with TR and trx. Each condition was incubated for four hours, and the samples were run in a non-reducing SDS-PAGE to visualize if CTA reduction had taken place.

CTA alone showed it was present and no reduced CTA was present; reduced CTA (CTA + βme) showed the position; CTA with PDI shows that TR and trx are required to reduce CTA, and CTA with TR and trx showed that PDI was required to reduce CTA. A band at the molecular weight corresponding to CTA1 signified that reduction had taken place (Fig. 15).The conditions with the molecular crowders showcased that no crowder inhibited reduction of CTA by PDI, therefore they didn't block the oxidoreductase properties of PDI. Even sucrose that had inhibited ELISA binding was not enough to inhibit reduction. That leads to the prediction that reduction of CTA by PDI required less stable binding.

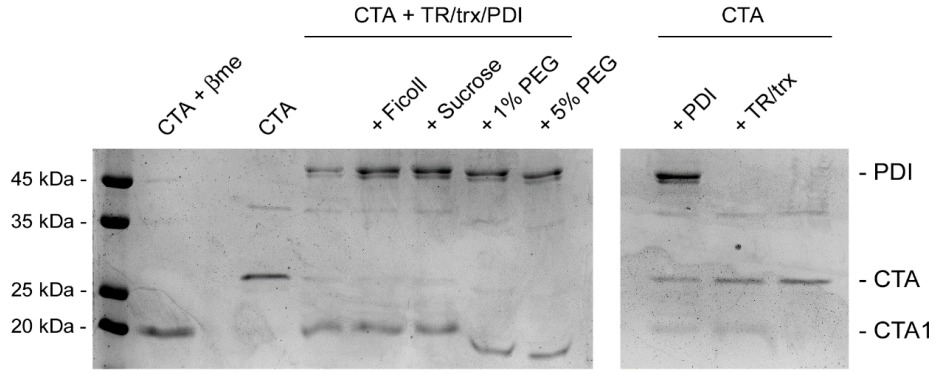

Figure 15: CTA reduction by PDI. Lanes were used to test if PDI and CT interaction was affected by molecular crowders. The samples were incubated for 4 hours at 37°C, where all PDI samples were reduced by NADPH/TR/Trx system (Fig. 11). The various samples were run on a 15% SDS-PAGE. One sample, rCTA was reduced completely by chemical treatment (βme), while the rest of the samples were nonreducing. One of two reproducible experiments is shown.

ELISA Disassembly Assay

This assay quantified the percent disassembly of CTA1 by PDI in the presence of various molecular crowders, and the results were compared to the control condition of no molecular crowders. Our initial hypothesis was that the molecular crowding agents would increase the efficiency of disassembly. Molecular crowding agents may provide an extra push by generating more collisions in general, hence enhancing the disassembly event.

A 96 well plate was coated with GM1 ganglioside, which is a receptor for CT. This is the same receptor found on cell surface of intestinal epithelial cells, making it a great method to capture CT on the plate. Thereafter, reduced PDI was added to allow it to disassemble CTA1. An antibody that recognizes CTA1 was added, followed by a secondary antibody that is HRP conjugated. The addition of its substrate allowed for the quantification of percent disassembly, where a loss in signal was interpreted as disassembly had occurred. Preliminary experiments reported that molecular crowders inhibit disassembly from occurring, as there is less disassembly when compared to the control (Fig. 16). The binding assay showed that sucrose inhibited PDI to bind to CTA1, so it made sense that its disassembly signal was very low. However, other crowding agents did not block binding, so another reason has to be present to explain a reduced disassembly event. A possible explanation for this observation is PDI's inability to unfold. The molecular crowders may favor a folded state of PDI rather than the unfolded state due to limited space to unfold and act as wedge for CTA1 disassembly. More repeats need to be conducted to establish reproducibility.

Other scientists have stated that molecular crowding agents destabilize proteins. Crowding agents cause the compaction of expanded protein structures by exerting a mechanical force on them. Furthermore, molecular crowders enhance undesirable protein aggregation, which destabilizes proteins[58].

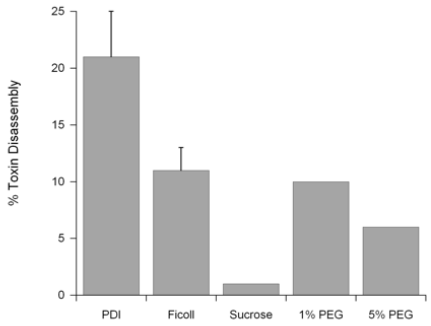

Figure 16: ELISA disassembly assay. CT was captured on the wells of a GM1-coated ELISA plate. PDI was added in the presence of the various molecular crowders, or with no crowders for the control. It's already known that PDI disassembles CTA1 in vitro, hence, all the other conditions were compared to this.

CONCLUSION

PDI and CT interactions have been thoroughly studied, but how they interact within the ER remains obscure. The importance of this thesis is to understand in vivo interactions in an in-vitro setting between PDI and CT. This will help scientists grasp a better insight of what really is happening on a physiologic level. Preliminary ELISA data suggests that CT disassembly is an inefficient process, in comparison to previous SPR data. This suggests that toxin disassembly is an inefficient process in the ER, and it is the high concentration of PDI within the ER that allows for CT disassembly, CTA1 activation and a severe cholera infection.

The WHO states that rehydration therapy is a good treatment for cholera infections. However, no treatments involve preventing CT from binding to PDI. If PDI-CT interactions are prevented, no cholera infection would be created. In the long term, this project could help with the design of cholera therapeutics.

FUTURE DIRECTIONS

Fist and foremost, more data needs to be generated using the ELISA assays to show that the preliminary data are reproducible. Secondly, SPR with molecular crowders is an independent method to follow CT disassembly which will ensure our results are reproducible. Furthermore, FTIR experiments are going to be conducted, where we predict molecular crowders may block the CTA1 induced unfolding of PDI.

Lastly, the pull down protocol needs to be polished before molecular crowders are introduced. All future experiments will not use sucrose, where the effect seen was not due to a lack of disassembly but a lack of binding.

REFERENCES

(1) Jacqueline Deen, M. A. M., John D Clemens. Epidemiology of cholera. *Vaccine* **2020**, *Volume 38, Supplement 1* (ISSN 0264-410X), Pages A31-A40.

(2) Ali, M. e. a. Updated global burden of cholera in endemic countries. *PLoS neglected tropical diseases* **2015**, *vol. 9* (6). DOI: doi:10.1371/journal.pntd.0003832.

(3) Cholera – Vibrio cholerae infection. Centers for Disease Control and Prevention.

(4) Cholera vaccines: WHO position paper. In *Weekly Epidemiological Record*, 25 August 2017; Vol. No 34.

(5) Shannon, K. e. a. Cholera prevention and control in refugee settings: Successes and continued challenges. *PLoS neglected tropical diseases* **2019**, *13* (6). DOI: doi:10.1371/journal.pntd.0007347.

(6) al., G. Q. e. Cholera Outbreak in Dadaab Refugee Camp, Kenya — November 2015–June 2016. MMWR Morb Mortal Wkly Rep: 2018; Vol. 67, pp 958–961.

(7) Jutla, A. e. a. Natural Disasters and Cholera Outbreaks: Current Understanding and Future Outlook. *Current environmental health reports* **2017**, *4* (1), 99-107. DOI: doi:10.1007/s40572-017-0132-5.

(8) Hadeed, S. J. e. a. Notional Spread of Cholera in Haiti Following a Natural Disaster: Considerations for Military and Disaster Relief Personnel. *Military Medicine* **2022**. DOI: https://doi.org/10.1093/milmed/usac415.

(9) Song, J. *Bacterial AB toxins and host–microbe interactions*; Advances in Microbial Physiology, 2022.

(10) Cherubin P, G. M., Curtis D, Britt CBT, Craft JW Jr, et al. Inhibition of Cholera Toxin and Other AB Toxins by Polyphenolic Compounds. *PLOS ONE* **2016**, *11* (11).

(11) Teter, K. Toxin instability and its role in toxin translocation from the endoplasmic reticulum to the cytosol. *Biomolecules* **2013**, *3* (4), 997-1029. DOI: doi:10.3390/biom3040997.

(12) Di Bella, S. e. a. Clostridium difficile Toxins A and B: Insights into Pathogenic Properties and Extraintestinal Effects. *Toxins* **2016**, *8* (5). DOI: doi:10.3390/toxins8050134.

(13) Callista B. Harper, A. M., Phillip J. Robinson, Frederic A. Meunier. *Exploiting endocytic pathways to prevent bacterial toxin infection*; Academic Press, 2015.

(14) Taylor, M. e. a. Protein-disulfide isomerase displaces the cholera toxin A1 subunit from the holotoxin without unfolding the A1 subunit. **2011**, *vol. 286,25*.

(15) Wernick, N. L. B. e. a.-. Cholera toxin: an intracellular journey into the cytosol by way of the endoplasmic reticulum. **2010**, *2*, 310-325.

(16) J J Mekalanos; R J Collier; W R Romig. Enzymic activity of cholera toxin. II. Relationships to proteolytic processing, disulfide bond reduction, and subunit composition. *Journal of Biological Chemistry* **1979**, *254* (13), 5855-5861. DOI: https://doi.org/10.1016/S0021-9258(18)50491-9.

(17) Jobling, M. G.; Holmes, R. K. Identification of motifs in cholera toxin A1 polypeptide that are required for its interaction with human ADP-ribosylation factor 6 in a bacterial two-hybrid system. *Proceedings of the National Academy of Sciences of the United States of America* **2000**, *97* (26). DOI: doi:10.1073/pnas.011442598.

(18) Massey, S. e. a. Stabilization of the tertiary structure of the cholera toxin A1 subunit inhibits toxin dislocation and cellular intoxication. *Journal of molecular biology* **2009**, *393* (5), 1083-1096. DOI: 10.1016/j.jmb.2009.09.013.

(19) Majoul, I. e. a. Reduction of protein disulfide bonds in an oxidizing environment. The disulfide bridge of cholera toxin A-subunit is reduced in the endoplasmic reticulum. *FEBS letters* **1997**, *401* (2-3), 104-108. DOI: doi:10.1016/s0014-5793(96)01447-0.

(20) Tsai, B. e. a. Protein Disulfide Isomerase Acts as a Redox-Dependent Chaperone to Unfold Cholera Toxin. *Cell* **2001**, *104* (6), 937 - 948.

(21) Guichard, A. e. a. Cholera toxin disrupts barrier function by inhibiting exocyst-mediated trafficking of host proteins to intestinal cell junctions. **2013**, *14*, 294-305.
(22) White, C. e. a. The manipulation of cell signaling and host cell biology by cholera toxin. *Cellular signalling* **2022**, *100* (110489). DOI: doi:10.1016/j.cellsig.2022.110489.
(23) al., T. B. e. Contribution of Subdomain Structure to the Thermal Stability of the Cholera Toxin A1 Subunit. *Biochemistry* **2010**, *49* (41), 8839–8846. DOI: https://doi.org/10.1021/bi101201c.
(24) Teter, K. e. a. Transfer of the cholera toxin A1 polypeptide from the endoplasmic reticulum to the cytosol is a rapid process facilitated by the endoplasmic reticulum-associated degradation pathway. *Infection and immunity* **2002**, *70* (11), 6166-6171. DOI: 10.1128/IAI.70.11.6166-6171.2002.
(25) Brodsky, J. L. The protective and destructive roles played by molecular chaperones during ERAD (endoplasmic-reticulum-associated degradation). *The Biochemical journal* **2007**, *404* (3), 353-363. DOI: 10.1042/BJ20061890.
(26) Teter, K. e. a. A class of mutant CHO cells resistant to cholera toxin rapidly degrades the catalytic polypeptide of cholera toxin and exhibits increased endoplasmic reticulum-associated degradation. **2003**, *vol. 4*, 232-242.
(27) Winkeler, A. e. a. BiP-dependent export of cholera toxin from endoplasmic reticulum-derived microsomes. *FEBS letters* **2003**, *554* (3), 439-442. DOI: 10.1016/s0014-5793(03)01217-1.
(28) Ciechanover, A.; Schwartz, A. L. The ubiquitin-proteasome pathway: the complexity and myriad functions of proteins death. *Proceedings of the National Academy of Sciences of the United States of America* **1998**, *95* (6), 2727-2730. DOI: 10.1073/pnas.95.6.2727.
(29) Rodighiero, C. e. a. Role of ubiquitination in retro-translocation of cholera toxin and escape of cytosolic degradation. *EMBO reports* **2002**, *3* (2), 1222-1227. DOI: 10.1093/embo-reports/kvf239.
(30) Burress, H. e. a. HSC70 and HSP90 chaperones perform complementary roles in translocation of the cholera toxin A1 subunit from the endoplasmic reticulum to the cytosol. *The Journal of biological chemistry* **2019**, *294* (32), 12122-12131. DOI: 10.1074/jbc.RA119.008568.
(31) Goodsell, D. *Molecule of the Month: Cholera Toxin*. 2005. (accessed.
(32) Wernick, N. L. B. e. a.-. Cholera toxin: an intracellular journey into the cytosol by way of the endoplasmic reticulum. *Toxins* **2010**, *2*, 310-325.
(33) Banerjee, T. e. a. cAMP-Independent Activation of the Unfolded Protein Response by Cholera Toxin. *Infection and immunity* **2021**, *89* (2). DOI: doi:10.1128/IAI.00447-20.
(34) Schwarz, D. S.; Blower, M. D. The endoplasmic reticulum: structure, function and response to cellular signaling. *Cellular and molecular life sciences* **2016**, *73*, 79-94. DOI: 10.1007/s00018-015-2052-6.
(35) Alberts B, J. A., Lewis J, et al. *Molecular Biology of the Cell*; Garland Science, 2002.
(36) Braakman, I., and Daniel N Hebert. Protein folding in the endoplasmic reticulum. *Cold Spring Harbor perspectives in biology* **2013**, *5* (5). DOI: doi:10.1101/cshperspect.a013201
(37) Weihofen, A. e. a. Identification of signal peptide peptidase, a presenilin-type aspartic protease. *Science (New York, N.Y.)* **2002**, *296* (5576), 2215-2218. DOI: 10.1126/science.1070925.
(38) Reid, D. W.; Nicchitta, C. V. Diversity and selectivity in mRNA translation on the endoplasmic reticulum. *Nature reviews Molecular cell biology* **2015**, *vol. 16* (4), 221-231. DOI: doi:10.1038/nrm3958.
(39) Puig, A.; F, G. H. Protein disulfide isomerase exhibits chaperone and anti-chaperone activity in the oxidative refolding of lysozyme. *The Journal of biological chemistry* **1994**, *269* (10), 7764-7771.
(40) Graner MW, L. K., Katsanis E. Endoplasmic reticulum chaperones and their roles in the immunogenicity of cancer vaccines. **2015**, *vol. 4* (379). DOI: doi:10.3389/fonc.2014.00379.
(41) T, G.; T, S. Endoplasmic reticulum chaperones and oxidoreductases: critical regulators of tumor cell survival and immunorecognition. *Front. Oncol.* **2014**, *4* (291). DOI: doi: 10.3389/fonc.2014.00291.

(42) Qi, L. e. a. New Insights into the Physiological Role of Endoplasmic Reticulum-Associated Degradation. *Trends in cell biology* **2017**, *VOL. 27* (6), 430-440. DOI: doi:10.1016/j.tcb.2016.12.002.
(43) Meusser, B.; Hirsch, C.; Jarosch, E. *e. a.* ERAD: the long road to destruction. *Nat Cell Biol* **2005**, *7*, 766–772.
(44) Biederer, T. e. a. Degradation of subunits of the Sec61p complex, an integral component of the ER membrane, by the ubiquitin-proteasome pathway. *The EMBO journal* **1996**, *15* (9), 2069-2076.
(45) Read, A.; Schröder, M. The Unfolded Protein Response: An Overview. *Biology* **2021**, *vol. 10* (5), 384. DOI: doi:10.3390/biology10050384.
(46) Ali Khan, H., and Bulent Mutus. Protein disulfide isomerase a multifunctional protein with multiple physiological roles. **26 Aug. 2014**, *vol. 2:70*. DOI: doi:10.3389/fchem.2014.00070.
(47) Ellgaard, L. e. a. How Are Proteins Reduced in the Endoplasmic Reticulum? **2018**, *vol. 43,1*, 32-43. DOI: doi:10.1016/j.tibs.2017.10.006.
(48) Fu, J. e. a. PDI-Regulated Disulfide Bond Formation in Protein Folding and Biomolecular Assembly. *Molecules (Basel, Switzerland)* **2020**, *26* (1). DOI: doi:10.3390/molecules26010171.
(49) Taylor, M. e. a. Protein-disulfide isomerase displaces the cholera toxin A1 subunit from the holotoxin without unfolding the A1 subunit. *The Journal of biological chemistry* **2011**, *vol. 286* (25).
(50) Taylor, M. e. a. Substrate-Induced Unfolding of Protein Disulfide Isomerase Displaces the Cholera Toxin A1 Subunit from Its Holotoxin. *Plos Pathogens* **2014**, *10* (2). DOI: 10.1371/journal.ppat.1003925.
(51) Ellis, R.; Minton, A. Join the crowd. *Nature* **2003**, (425), 27-28.
(52) Benny, P.; Raghunath, M. Making microenvironments: A look into incorporating macromolecular crowding into in vitro experiments, to generate biomimetic microenvironments which are capable of directing cell function for tissue engineering applications. *Journal of tissue engineering* **2017**, *vol. 2*. DOI: doi:10.1177/2041731417730467.
(53) Christiansen, A. e. a. Effects of macromolecular crowding agents on protein folding in vitro and in silico. *Biophysical reviews* **2013**, *vol. 5* (2), 137-145. DOI: doi:10.1007/s12551-013-0108-0.
(54) Damien Hall, A. P. M. Macromolecular crowding: qualitative and semiquantitative successes, quantitative challenges. *Biochimica et Biophysica Acta (BBA) - Proteins and Proteomics* **2003**, *1649* (2), 127-139.
(55) Fulton, A. B. How crowded is the cytoplasm. *Cell* **1982**, *30*, 345-347. DOI: 10.1016/0092-8674(82)90231-8.
(56) Zimmerman, S. B., and A P Minton. Macromolecular crowding: biochemical, biophysical, and physiological consequences. *Annual review of biophysics and biomolecular structure* **1993**, *22*, 27-65. DOI: doi:10.1146/annurev.bb.22.060193.000331.
(57) Krause, G. e. a. Mimicking the active site of protein disulfide-isomerase by substitution of proline 34 in Escherichia coli thioredoxin. *The Journal of biological chemistry* **1991**, *266* (15), 9494-9500.
(58) al., D.-L. Z. e. Effects of macromolecular crowding on the structural stability of human α-lactalbumin. *Acta Biochimica et Biophysica Sinica* **2012**, *44* (8), 703–711. DOI: https://doi.org/10.1093/abbs/gms052.